

# Electrochemical Detection of Methyl Parathion in *Fritillaria thunbergii* Based on Acetylcholinesterase Immobilized Gold Nanosphere

Jianwei Jiang, Hongyan Zhang, Chunlei Wang\* and Ying Xu

The Department of Pharmacy, Zhejiang Cancer Hospital, 38 Guangji Rd, Gongshu, Hangzhou, Zhejiang, 310022, P.R. China

\*E-mail: [chunleiwang\\_zch@yeah.net](mailto:chunleiwang_zch@yeah.net)

Received: 1 April 2016 / Accepted: 19 May 2016 / Published: 4 June 2016

---

Large use of pesticide is an important issue in modern agriculture. Development of a reliable analytical method for pesticide detection is essential for many fields. In this work, we proposed an electrochemical based detection method for methyl parathion, an organophosphate pesticide, residue in the *Fritillaria thunbergii*, a medicinal plant has been cultivated for several thousand years, based on the acetylcholinesterase immobilized gold nanosphere (Au NS) modified electrode. The combination of acetylcholinesterase and Au NS displayed a strong synergetic effect on enhancing the detection properties of methyl parathion. Au NS could catalyze the oxidation process of the enzymatically produced thiocholine and result a high sensitivity. After optimization, the proposed biosensor was used for analyzing the methyl parathion residue in freshly harvested *Fritillaria thunbergii*.

---

**Keywords:** Pesticide; Methyl parathion; *Fritillaria thunbergii*; Gold nanosphere; Acetylcholinesterase

## 1. INTRODUCTION

*Fritillaria thunbergii*, Zhebei in Chinese, has been used as an antitussive and expectorant medicinal plant in Chinese medicine for more than two thousand years. For now, growth and cultivation of *Fritillaria thunbergii* become a mature market in many Asian countries including China, Taiwan and Japan. However, the use of organophosphorous pesticides for pest control is a common method for enhancing the harvest of the *Fritillaria thunbergii*. Organophosphorous pesticides exhibit high toxicity and irreversibly inhibition of acetylcholinesterase, which commonly occurs serious health issues such as respiratory paralysis and death [1]. Thus, the development of a rapid and reliable analytical method for trace amount of organophosphorous pesticide determination is very important for environmental and health protection. So far, GC-MS and HPLC have been commonly used for

organophosphorous pesticide determination [2-8]. However, these methods need complicated sample preparation and operation process. Moreover, the instrument limitation makes them cannot be applied for on-site determination.

Electrochemical approach has been to find satisfy many of the current analytical requirements due to its simplicity, excellent stability, high selectivity and low cost [9-13]. Especially, enzyme-based electrochemical determination process showed excellent performance for organophosphorous pesticide determination [14-17]. Among the enzymes, acetylcholinesterase (AChE) has been found specifically targeting the determination of organophosphorous pesticide as an indicator [18-20]. AChE is an enzyme that keeps the acetylcholine levels in neuro-system through the acetylcholine hydrolysis to thiocholine. The presence of organophosphorous pesticide could inhibit the catalytic activity of AChE and can be detected by electro-signal. Usually, the application of AChE on organophosphorous pesticide was through direct electrode surface immobilization. However, this approach always leads to the inefficiency of AChE immobilization due to weak protection of the AChE. How to remain the bioactivity of the AChE after immobilization also is a great challenge for designing AChE based electrochemical sensor.

Some nanomaterials for example Au NPs, Pd NPs, Pd NPs have been used in the electrochemical biosensor fabrication. Among these nanomaterials, Au NPs showed promising catalytic ability to enhance the electrochemical property of commercial electrode. Therefore, Au NPs could be applied as the immobilization matrix for the design AChE based electrochemical biosensor. Despite the solid Au NPs, hollow gold nanospheres (Au NS) also received great attention. Zhong and co-workers demonstrated the synthesis of Au NS using a template method and then successfully applied for chemiluminescence glucose detection [21].

In this work, we demonstrated the synthesis of well-distributed hollow Au NS for encapsulating AChE using a simple template method. The synthesized Au NS showed a large surface area, excellent conductivity and biocompatibility. The enhancement of loading AChE was observed at the Au NS with remaining of bioactivity. Methyl parathion was chosen as an organophosphorous pesticide model for electrochemical analysis. The combination of Au NS with AChE largely enhanced the oxidation of AChE generated thiocholine, which enhancing the detection sensitivity. The parameters of the detection process were optimized and the detection range was investigated in detail. In addition, the proposed biosensor was used for detecting methyl parathion residue in freshly harvested *Fritillaria thunbergii*.

## 2. EXPERIMENTS

### 2.1. Materials

Hydrogen tetrachloroaurate ( $\text{HAuCl}_4 \cdot 4\text{H}_2\text{O}$ ),  $\text{Na}_3\text{C}_6\text{H}_5\text{O}_7 \cdot 2\text{H}_2\text{O}$ ,  $\text{NaBH}_4$ , pralidoxime iodide, acetylcholinesterase, acetylthiocholine chloride, methyl parathion and  $\text{CoCl}_2 \cdot 6\text{H}_2\text{O}$  were purchased from Sigma. All other reagents were of analytical grade and used without further purification. Milli-Q

water was used through all experiments. Phosphate buffered solution (PBS) (pH 7.4, 0.1 M) was prepared by mixing  $\text{Na}_2\text{HPO}_4$  with M  $\text{KH}_2\text{PO}_4$ .

## 2.2. Synthesis of Au NS

Au NS was synthesized according to Schwartzberg's report with some modification. Typically, 200  $\mu\text{L}$  of  $\text{Na}_3\text{C}_6\text{H}_5\text{O}_7 \cdot 2\text{H}_2\text{O}$  (0.1 M) was added into 100 mL water under stirring in the  $\text{N}_2$  condition. Then, 100  $\mu\text{L}$  of an ice-cooled  $\text{NaBH}_4$  (1 M) and 50  $\mu\text{L}$   $\text{CoCl}_2 \cdot 6\text{H}_2\text{O}$  (0.5 M) were subsequently added. The colour change of the solution can be visually observed. After half hour stirring, 150  $\mu\text{L}$  0.1 M  $\text{HAuCl}_4$  solution was slowly introduced for Au NS formation. The dispersion was further stirred for an additional hour in order to oxidase the residue Co. Centrifugation and water wash process was carried out for the dispersion. The resultant Au NS was dispersed in water for further use.

## 2.3. Electrode modification

Prior to surface modification, the bare glassy carbon electrode (GCE) was polished using 0.3 and 0.05  $\mu\text{m}$  alumina slurry and washed by water and ethanol. After remove any adsorbed impurities, certain amount of the Au NS (0.5 mg/mL) dispersion was dropped on the GCE surface and then dried at room temperature. Au NS/GCE was then coated with 5  $\mu\text{L}$  of AChE solution and incubated at 25  $^\circ\text{C}$  for half hour to result the Au NS-AChE/GCE.

## 2.4. Characterization

Morphology of synthesized Au NS was observed by transmission electron microscope (TEM, Hitachi H-7500, Japan). The UV-vis spectrum of the Au NS was recorded at a UV-vis spectrophotometer (HALO RB-10, Dynamica). X-ray photoelectron spectroscopy (XPS, VG Sigma Probe) were applied to investigate the surface chemical status of the formed Au NS. For methyl parathion determination, 1 mM acetylthiocholine chloride was added into PBS for measurement. The inhibition of methyl parathion can be determined for analyzing the performance of Au NS-AChE/GCE using the follow equation:

$$\text{Inhibition}(\%) = \frac{I_c - I_e}{I_c} \times 100$$

where  $I_c$  is the peak current of acetylthiocholine chloride on the Au NS-AChE/GCE without adding of methyl parathion;  $I_e$  is the peak current of acetylthiocholine chloride on the Au NS-AChE/GCE when the presence of methyl parathion.

## 2.5. Electrochemical determination

All electrochemical characterizations and determinations were carried out at a CHI 660A Electrochemical Workstation from Shanghai Chenhua Instrument and conducted using a three-

electrode system, with the modified GCE as working electrode, a platinum wire as the counter electrode, a 3 M Ag/AgCl electrode as the reference electrode. Electrochemical impedance spectroscopy (EIS) was used for characterizing the electrode resistance performance. 5 mM  $[\text{Fe}(\text{CN})_6]^{3-/4-}$  was used as probe, 0.1 M KCl was used as supporting electrolyte. Frequency range was set as  $10^1$  to  $10^5$  Hz and the amplitude was set as 5 mV. CV was performed in 0.1 M pH 7.0 PBS from 0 to 1.0 V at scan rate of 50 mV/s. The effect of pH condition was carried out by CV method at 0.1 M PBS with different pH conditions. The effect of the inhibition time was carried out by immersing Au NS-AChE/GCE into acetylthiocholine chloride containing PBS by different period before CV scan. The effect of the temperature was performance at an incubator with different temperature conditions.

### 3. RESULTS AND DISCUSSION

The morphology of the synthesized Au NS was characterized using TEM. Figure 1A shows the typical TEM image of Au NS. It can be seen that the Au NS exhibits an excellent dispersibility with an average size of XXX nm. The hollow structure can be distinguished by the contrast difference between Au shells with carbon holder film. UV-vis spectrometer was then used for characterizing the formed Au NS. Figure 1B shows the spectrum of Au NS dispersion, which showed a well-defined adsorption peak at 530 nm due to the surface plasmon absorption of the Au NS. Therefore, the TEM observed nano-sphere was confirmed to be Au NS. XPS was used for further confirming the formation of Au NS. Figure 1C shows the Au 4f XPS spectrum of Au NS. As shown in the spectrum, the Au 4f<sub>7/2</sub> peak was observed at a binding energy of 84.13 eV and the Au 4f<sub>5/2</sub> peak was observed at a binding energy of 87.89 eV, further suggesting the formation of metallic gold [22, 23].

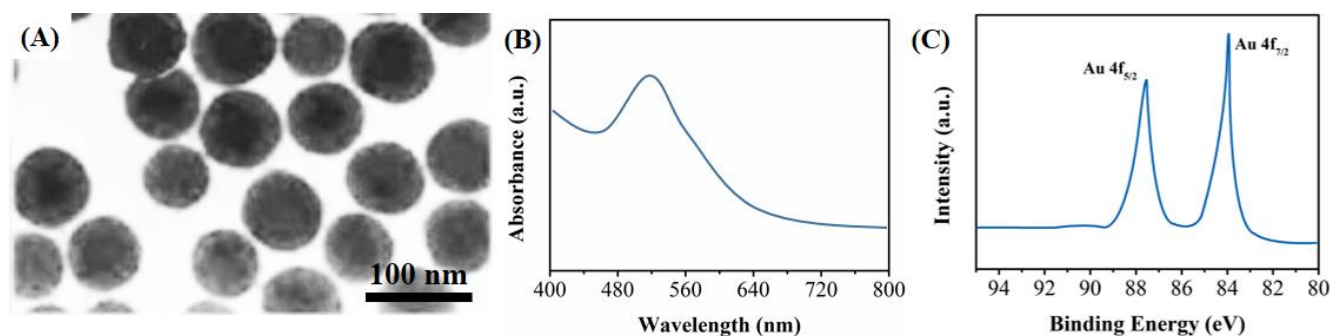


**Figure 1.** (A) TEM image and (B) UV-vis spectrum of Au NS. (C) Au 4f XPS spectrum of Au NS.

The electrochemical behaviours of the Au NS and Au NS-AChE were studied using electrochemical impedance spectroscopy (EIS) and cyclic voltammetry (CV). EIS result could provide information about the interfacial changes of the electrode. The semicircle part observed at high frequencies in Nyquist plot is related to the charge transfer limiting process. Figure 2A shows the impedance spectra of bare GCE, Au NS/GCE, AChE/GCE and Au NS-AChE/GCE in  $\text{K}_3\text{Fe}(\text{CN})_6/\text{K}_4\text{Fe}(\text{CN})_6(1:1)$  solution (0.1 M KCl). It can be seen that the surface immobilization of

AChE on the bare GCE remarkably increased the charge transfer resistance of the electrode. On the other hand, Au NS modified GCE dramatically decreased the charge transfer resistance due to the excellent electronic property of Au NS. The plot of Au NS-AChE/GCE show a larger charge transfer resistance than Au NS/GCE but much lower than that of the bare GCE and AChE/GCE. Therefore, the combination of the Au NS and AChE could effectively enhance the electrochemical performance of the electrode.

CV was also used for analysing the electrochemical performance of the electrodes. Figure 2B shows the CV scans in 5.0 mM  $K_3Fe(CN)_6/K_4Fe(CN)_6(1:1)$  solution (0.1 M KCl). A well-defined redox peaks were recorded at bare GCE. When AChE deposited on the GCE, the electrode showed a wider peak-to-peak potential distance with decreased peak current values. In contrast, peak currents increased was recorded on the Au NS/GCE due to the excellent electrochemical property of Au nanomaterials. After further surface immobilization of AChE, the Au NS-AChE/GCE showed a slightly decreasing in peak current, which in a good agreement with the result recorded on the EIS.

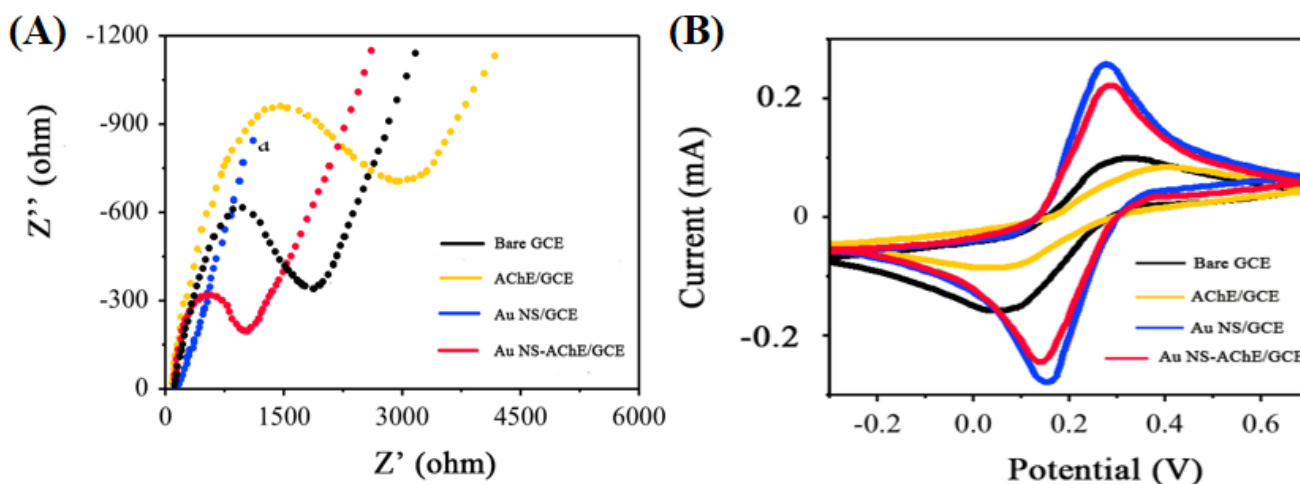


**Figure 2.** (A) Nyquist diagrams and (B) CV profiles of bare GCE, Au NS/GCE, AChE/GCE and Au NS-AChE/GCE in 5 mM  $K_4[Fe(CN)_6]$  + 0.1 M KCl.

Figure 3A shows the CV profiles of bare GCE, Au NS/GCE, AChE/GCE and Au NS-AChE/GCE towards 1 mM acetylthiocholine chloride. As shown in the figure, no detectable signal was recorded on the bare GCE and Au NS/GCE, suggesting the acetylthiocholine chloride cannot be hydrolyzed on the common electrode. In contrast, a clear peak related to the thiocholine oxidation was recorded at AChE/GCE and Au NS-AChE/GCE due to the catalysis of acetylthiocholine chloride by immobilized AChE. The electrochemical response of acetylthiocholine chloride at Au NS-AChE/GCE showed a significant enhancement compared with that of AChE/GCE due to the presence of Au NS on the electrode. Moreover, the over potential of the oxidation peak showed a negative shift, suggesting the Au NS not only contributes the excellent conductivity but also catalyzed the surface chemical reaction. Therefore, the Au NS provides an excellent immobilization platform for AChE and prompts the electron transport on the electrode.

We then introduced the methyl parathion into the above system for organophosphorous pesticide detection performance analysis. Figure 3B shows the CV profiles of Au NS-AChE/GCE towards different concentrations of methyl parathion in 1 mM acetylthiocholine chloride. It can be seen that the peak current decreased drastically when the concentration of methyl parathion increasing. The decreasing of the peak current can be ascribed to the high toxicity of the methyl parathion, resulting an in irreversible inhibition process of AChE. Because the enzymatic activity inhibition degree of the AChE can be related to the concentration of the methyl parathion, the proposed biosensor can be used for quantitative methyl parathion determination.

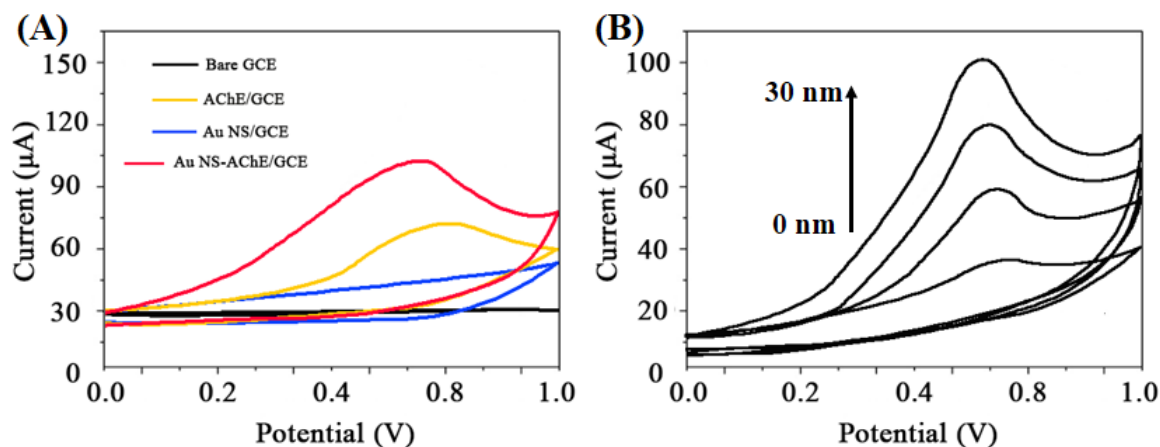


**Figure 3.** (A) Cyclic voltammograms of bare GCE, Au NS/GCE, AChE/GCE and Au NS-AChE/GCE towards 1 mM acetylthiocholine chloride in 0.1 M PBS. Scan rate: 50 mV/s. (B) Cyclic voltammograms of bare GCE, Au NS/GCE, AChE/GCE and Au NS-AChE/GCE towards different concentrations of methyl parathion (0, 10, 20 and 30 nM) in the PBS containing 1 mM acetylthiocholine chloride.

The bioactivity of the AChE is related to the pH condition of the detection system. Figure 4a shows the effect of the pH on the peak current of acetylthiocholine chloride. The peak current response increased when the pH value increased from 4 to 7 and reached the maximum value at pH 7. Further increasing of pH showed decreasing of the current response. Therefore, pH 7 of PBS was chosen for methyl parathion detection.

We then optimized the influence of inhibition time of the Au NS-AChE/GCE towards acetylthiocholine chloride detection. Figure 4B shows the relationship between current response and inhibition time. It can be seen that the peak current of acetylthiocholine chloride decreased when the Au NS-AChE/GCE immersed into methyl parathion solution from 1 to 8 min. After 8 min, the current response showed a stable value, suggesting the inhibition process reached maximum within 8 min. Therefore, 8 min was chosen as optimum inhibition time.

The temperature also could affect the bioactivity of the AChE. Figure 4C shows the current responses of the Au NS-AChE/GCE towards acetylthiocholine chloride detection at various temperatures. A clear increase tendency of peak response was observed on the Au NS-AChE/GCE from 0 to 24  $^{\circ}\text{C}$ . Whereas, with the temperature increased from 24 to 40  $^{\circ}\text{C}$ , no obvious decrease in

response was observed, suggesting that the immobilization of AChE at Au NS could retained its bioactivity at wide temperature range. For practical convenience, 25 °C was chosen for all detection experiment.

As mentioned above, the current response of Au NS-AChE/GCE towards acetylthiocholine chloride can be affected by the amount of methyl parathion present in the system. We then studied the detection range of the proposed methyl parathion biosensor under optimized experimental conditions. Figure 5 shows the inhibition efficiency of the Au NS-AChE/GCE with different concentrations of methyl parathion. As shown in the figure, the 92.6% inhibition will occur when the concentration of methyl parathion exceeds 0.3 μM. Two linear detection ranges were recorded on the measurements, from 0.5 to 25 nM and 25 to 300 nM. The detection limit of the proposed methyl parathion biosensor was estimated to be 0.12 nM based on signal to noise of 3. The detection limit obtained is comparable with that reported so far with an enzyme-based inhibitor electrochemical sensor [24], and it is significantly lower than those of 13.2 nM at carbon paste electrode by using stripping analysis [25], and also lower than 4.8 nM at the hanging mercury drop electrode [26], indicating that the proposed Au NS-AChE/GCE is reliable for the determination of methyl parathion.

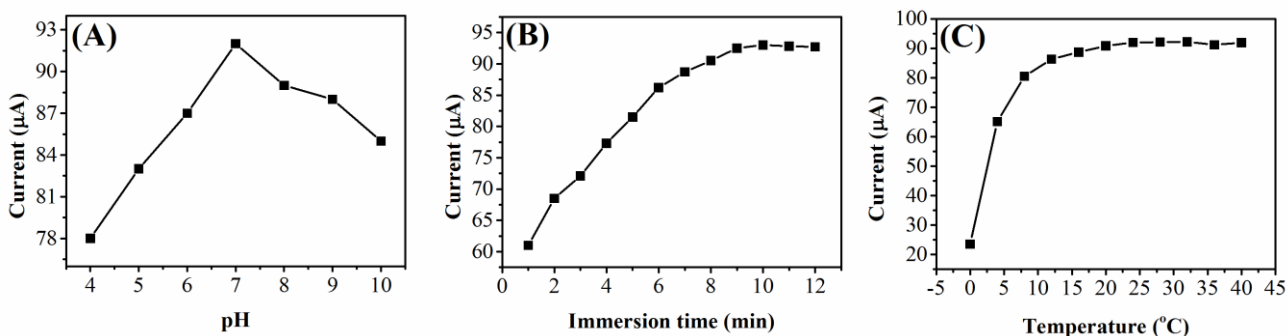


**Figure 4.** Effects of (A) pH, (B) immersion time and (C) temperature on the electrochemical response of the Au NS-AChE/GCE.

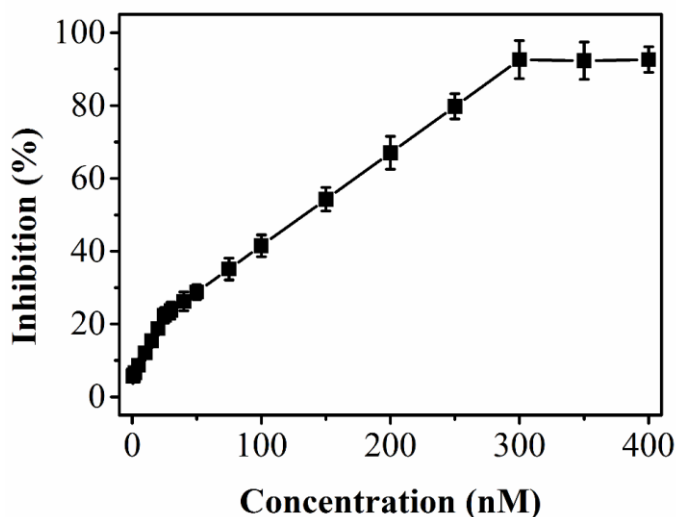


**Figure 5.** Plots of methyl parathion concentrations with inhibition efficiency using Au NS-AChE/GCE.

We further investigated the real application performance of proposed Au NS-AChE/GCE by determination of methyl parathion in freshly harvested *Fritillaria thunbergii*. Four batches of *Fritillaria thunbergii* were purchased from local Chinese herbal medicine market. The fresh *Fritillaria thunbergii* was crushed using a blender and the extract was filtrated. Standard addition method was used during the test. Table 1 shows the analyzed methyl parathion content in plant sample. It can be seen that only small amount of methyl parathion was detected in one sample. Excellent recovery result was observed for all samples. Therefore, the proposed Au NS-AChE/GCE had a good potential for developing as an on-site methyl parathion biosensor for real sample test.

**Table 1.** Determination of methyl parathion in *Fritillaria thunbergii* using Au NS-AChE/GCE.

Sample No.	Added (nM)	Found (nM)	Recovery (%)
1	0	0	—
	2	1.96	98.0
2	0	0	—
	10	10.30	103.00
3	0	2.15	—
	20	21.99	99.28
4	0	0	—
	50	50.21	100.42

The inhibition of AChE by methyl parathion can be reactivated by the treatment of pralidoxime iodide. After immersion of used Au NS-AChE/GCE into 1 mM pralidoxime iodide. The current response showed a recovery of 90 % compared with that of the original current response. Based on this observation, the proposed Au NS-AChE/GCE can be easily reused.

#### 4. CONCLUSION

A highly sensitive methyl parathion electrochemical biosensor was fabricated on the Au NS-AChE modified GCE. A stable and high efficiency of AChE immobilization was achieved on the Au NS. The proposed Au NS-AChE/GCE showed excellent performance towards detection methyl parathion through inhibition of the reaction between AChE and acetylthiocholine chloride. Two linear detection ranges were recorded on the established biosensor. The Au NS-AChE/GCE was successfully applied for methyl parathion detection in fresh harvested *Fritillaria thunbergii*. Moreover, the proposed methyl parathion can be reused through a simple reactivation process.

#### Reference

1. T. Kim, K. Kuca, D. Jun and Y. Jung, *Bioorg Med Chem Lett*, 15 (2005) 2914
2. S. Samadi, H. Sereshti and Y. Assadi, *Journal of Chromatography A*, 1219 (2012) 61
3. C. Hu, M. He, B. Chen and B. Hu, *Journal of Chromatography A*, 1275 (2013) 25



4. M.Á. González-Curbelo, J. Hernández-Borges, T.M. Borges-Miquel and M.Á. Rodríguez-Delgado, *Journal of Chromatography A*, 1313 (2013) 166
5. X. Zhao, W. Kong, J. Wei and M. Yang, *Food chemistry*, 162 (2014) 270
6. H. Heidari and H. Razmi, *Talanta*, 99 (2012) 13
7. K. Seebunrueng, Y. Santaladchaiyakit and S. Srijaranai, *Chemosphere*, 103 (2014) 51
8. J. Akan, O. Sodipo, Z. Mohammed and F. Abdulrahman, *Journal of Analytical & Bioanalytical Techniques*, 2014 (2014)
9. Y. Zheng, A. Wang, H. Lin, L. Fu and W. Cai, *RSC Advances*, 5 (2015) 15425
10. Y. Zheng, L. Fu, A. Wang and W. Cai, *Int. J. Electrochem. Sci*, 10 (2015) 3530
11. L. Fu, S. Yu, L. Thompson and A. Yu, *RSC Advances*, 5 (2015) 40111
12. L. Fu, G. Lai and A. Yu, *RSC Advances*, 5 (2015) 76973
13. L. Fu, G. Lai, B. Jia and A. Yu, *Electrocatalysis*, 6 (2015) 72
14. I. Gill and A. Ballesteros, *Biotechnology and bioengineering*, 70 (2000) 400
15. X. Meng, J. Wei, X. Ren, J. Ren and F. Tang, *Biosensors and Bioelectronics*, 47 (2013) 402
16. Y. Zhang, M.A. Arugula, M. Wales, J. Wild and A.L. Simonian, *Biosensors and Bioelectronics*, 67 (2015) 287
17. P.B. Dennis, A.Y. Walker, M.B. Dickerson, D.L. Kaplan and R.R. Naik, *Biomacromolecules*, 13 (2012) 2037
18. M. Kesik, F.E. Kanik, J. Turan, M. Kolb, S. Timur, M. Bahadir and L. Toppare, *Sensors and Actuators B: Chemical*, 205 (2014) 39
19. F. Arduini, S. Guidone, A. Amine, G. Palleschi and D. Moscone, *Sensors and Actuators B: Chemical*, 179 (2013) 201
20. J. Yan, H. Guan, J. Yu and D. Chi, *Pesticide Biochemistry and Physiology*, 105 (2013) 197
21. X. Zhong, Y.-Q. Chai and R. Yuan, *Talanta*, 128 (2014) 9
22. M. Seah, G. Smith and M. Anthony, *Surface and interface analysis*, 15 (1990) 293
23. T.D. Thomas and P. Weightman, *Physical Review B*, 33 (1986) 5406
24. E. Suprun, G. Evtugyn, H. Budnikov, F. Ricci, D. Moscone and G. Palleschi, *Anal Bioanal Chem*, 383 (2005) 597
25. G. Liu and Y. Lin, *Electrochemistry communications*, 7 (2005) 339
26. Y. Ni, P. Qiu and S. Kokot, *Anal. Chim. Acta.*, 516 (2004) 7